TOWARDS SYNERGISTIC ENERGY EFFICIENCY AND STABILITY IN MULTI-OBJECTIVE OPTIMIZED STEAM PRESSURE CONTROL SYSTEMS

Xiaolin GAO[1], Jing LU[2], Wenhao SHAO[3], Xiangmao YU[4], Xi CHEN[5,*], Zhihong HUANG[6]

This paper addresses the problem of the difficulty in achieving coordinated optimization of energy efficiency and stability in the steam pressure control of industrial boilers. It proposes a collaborative control strategy based on multi-objective optimization. By constructing a stability objective function measured by the ITAE index and an energy efficiency objective function centered on the integral of the rate of change of the control quantity and introducing actual constraints such as pressure fluctuation range and valve physical limits, a multi-objective optimization mathematical model for steam pressure is established. Combined with the NSGA-II multi-objective evolutionary algorithm, the parameters of the PID controller are optimized in a Pareto sense for collaborative control, and an optimized solution set that balances dynamic performance and energy-saving effect is obtained. On this basis, an online parameter scheduling strategy based on adaptive operating conditions is proposed. Combined with a hierarchical hardware architecture and a modular software platform, a steam pressure control system with real-time optimization capabilities is constructed. Simulation and experimental results show that this strategy ensures the rapid response and stability of the system while smoothing the actions of the actuator, significantly reducing energy loss during the control process, and provides a feasible theoretical method and engineering implementation path for solving multi-objective control conflicts in industrial processes.

Keywords: Steam pressure control, energy efficiency, stability, multi-objective optimization, NSGA-II algorithm

1. Introduction

Industrial boilers, as the core power source of process industries, the performance of their steam pressure control system directly affects the safety, stability and energy efficiency of the entire production process [1]. An ideal steam pressure control system not only needs to maintain pressure stability quickly and smoothly under load changes or external disturbances but also should minimize the energy consumption caused by the control action itself, thereby achieving the dual goals of "controllable" and "efficient control".

[1] Heilongjiang University of Technology, Heilongjiang, Jixi, China, 252659020@163.com
[2] Heilongjiang University of Technology, Heilongjiang, Jixi, China, 507485999@qq.com
[3] Heilongjiang University of Technology, Heilongjiang, Jixi, China, 2012253828@qq.com
[4] Heilongjiang University of Technology, Heilongjiang, Jixi, China, 3466958104@qq.com
[5] *Heilongjiang University of Technology, Heilongjiang, Jixi, China, 381975949@qq.com
[6] Heilongjiang University of Technology, Heilongjiang, Jixi, China, 1264076105@qq.com

Traditional research and practice on steam pressure control mainly focused on improving the dynamic response performance and stability of the system. For example, by adopting PID control and various improved algorithms, designers aimed to reduce system overshoot and shorten the regulation time to meet strict process safety requirements [2]. However, this optimization paradigm with a single stability goal has inherent limitations. To achieve rapid response, controllers often output highly variable control signals, driving the actuating mechanisms such as regulating valves or variable frequency pumps to frequently start and stop and make large movements. This "aggressive" control behavior will, on the one hand, exacerbate the mechanical wear of the actuators and shorten the equipment lifespan; on the other hand, the frequent actions of the valve drive devices consume more electrical energy or compressed air, and the rapid and large fluctuations in valve position will disrupt the steady state balance of the combustion system and steam-water system, reducing the overall thermodynamic efficiency[3].

In recent years, multi-objective optimization algorithms have been increasingly applied in complex industrial process control, providing new ideas for solving such trade-off problems. For example, Molina et al. [4] used multi-objective optimization technology to coordinate the energy efficiency and steam flow of a sugarcane residue boiler; Marques et al. [5] explored the tuning of a gain scheduling controller based on multi-objective evolutionary algorithms. These studies have confirmed that multi-objective optimization methods have advantages over single-objective methods when dealing with conflicting performance indicators. Most existing research is still at the stage of simulation verification and lacks engineering practice of integrating optimization algorithms, control system hardware and software platforms.

Compared with existing NSGA-II PID optimization studies, the main innovations of this work are reflected in the following aspects. A comprehensive multi-objective optimization framework that simultaneously considers system stability and energy efficiency is established, breaking through the limitations of traditional single-objective optimization. An online parameter scheduling strategy based on operating condition adaptation is proposed, achieving dynamic adjustment of controller parameters under different working conditions. A complete hardware and software integrated control system is designed and implemented, bridging the gap between optimization algorithms and engineering applications. The energy efficiency objective function is innovatively designed using the integral of the rate of change of control quantity, effectively quantifying the energy consumption during the control process.

To address the research gaps mentioned above, this paper aims to design and implement a steam pressure collaborative control system that integrates multi-objective offline optimization and online adaptive scheduling. The core objective of this study is to break through the limitations of single-objective optimization and, by

establishing a collaborative strategy, find the optimal balance point between energy efficiency and stability in the sense of Pareto optimality.

2. Multi-objective optimization model and design of Collaborative control strategy

A. System Energy Efficiency - Stability Analysis

In the steam pressure control system of industrial boilers, the pursuit of high-performance control strategies often requires a trade-off between dynamic quality and operational economy. Traditional single-objective optimization typically focuses on enhancing the stability and dynamic response performance of the system, such as reducing overshoot and shortening the regulation time, which are crucial for ensuring safety and process requirements [6]. However, this extreme pursuit of dynamic performance often leads to drastic changes in control commands, causing the regulating valve or variable frequency pump, as the main actuating mechanism, to frequently start and stop and make large movements. This "aggressive" control not only exacerbates the mechanical wear of the actuating mechanism, shortens the equipment lifespan, but also directly translates into considerable energy loss [7]. On one hand, the frequent actions of the valve drive device consume more electrical energy or compressed air; on the other hand, the rapid and significant fluctuations in valve opening disrupt the steady state balance of the combustion and steam-water system, reducing the overall thermodynamic efficiency [8]. Therefore, the energy efficiency of the system not only lies in the full combustion of fuel but is deeply embedded in the dynamic process guided by the control strategy, manifested as the smoothness of the actuating mechanism's actions and the minimization of control energy consumption.

Thus, there is an inherent coupling and conflict relationship between the intrinsic energy efficiency and stability goals within the system. A stability-optimal control with rapid response and small overshoot often has a highly variable control output, which is not conducive to energy efficiency; conversely, an overly "gentle" control that pursues absolute smoothness, although energy-saving, sacrifices response speed and disturbance resistance, resulting in slow system regulation and persistent deviations, unable to meet the stability requirements[9]. This competing contradiction relationship constitutes a typical multi-objective optimization problem in steam pressure control. The core of this study is to break the limitations of single-objective optimization, no longer considering energy efficiency and stability as mutually isolated indicators, but establishing a collaborative strategy to find the best balance point between the two in the sense of Pareto optimality, thereby ensuring that the dynamic quality of the system meets the process requirements while minimizing the energy loss caused by the control process, achieving the unity of economy and stability.

B. Energy Efficiency Objective Function Design

1) Design of stability objective function

The design of the stability objective function aims to convert the dynamic performance requirements of the system into quantifiable mathematical indicators [10]. To comprehensively evaluate the response quality of the system and avoid the limitations of a single indicator, this paper adopts the ITAE time-weighted absolute error integral criterion as the stability objective function. The ITAE criterion comprehensively reflects the changes of system errors over time in an integrated form through an integral form, and its mathematical expression is as follows:

$$J_{stability}=\int_0^T t\cdot|e(t)|dt \tag{1}$$

Among them, e(t) represents the system error at time t , which is the difference between the set pressure value and the actual value. T is the total time of the adjustment process. This formula introduces a time-weighting factor *t* to impose a higher penalty on the errors in the later stage of the transition process, thereby effectively suppressing system overshoot and oscillation, and enabling the response to quickly and smoothly approach the steady state. Compared with the ISE or IAE criteria, the ITAE criterion can better balance the response speed and stability, and the optimized result is more in line with the actual requirements for dynamic performance in industrial applications. The value of the objective function $J_{stability}$ is smaller, indicating that the comprehensive stability of the system is better.

2) Energy efficiency objective function design

The design of the energy efficiency objective function aims to quantify the energy consumption during the control process, with a focus on reflecting the impact of the action characteristics of the actuator on the system's energy efficiency [11]. Considering that the energy consumption of actuators such as control valves is directly related to their action amplitude and frequency, this paper adopts the integral of the rate of change of the control quantity as the energy efficiency evaluation index, and its mathematical expression is as follows:

$$J_{energy}=\int_0^T \left(\frac{du(t)}{dt}\right)^2 dt \tag{2}$$

Among them, u(t) represents the output of the control quantity at time *t,* which is the opening command of the regulating valve, and *T* is the operating period. This function integrates the square of the rate of change of the control quantity, effectively punishing drastic and frequent valve actions, and enabling the system to reach the control target in a smoother and more energy-efficient manner. The value of the objective function J_{energy} is smaller, indicating lower energy loss during the control process and better energy efficiency performance of the system. This design transforms the abstract concept of energy efficiency into specific mathematical indicators that can be optimized, providing a quantitative basis for multi-objective collaborative optimization.

3) Constraint conditions are determined

To ensure the feasibility and security of the optimization results in the actual system, corresponding constraints need to be established. This paper mainly considers two key constraints: the pressure fluctuation range constraint ensures that the system operation meets the process requirements, and the valve physical limit constraint guarantees the normal operation of the actuator [12]. The mathematical expressions are as follows: Pressure fluctuation range constraint:

$$P_{min} \leq P(t) \leq P_{max} \tag{3}$$

Among them, P(t) represents the measured steam pressure at time t, while P_{min} and P_{max} represent the minimum and maximum allowable pressure values as specified by the process requirements.

Physical limit constraints of the valve:

$$u_{min} \leq u(t) \leq u_{max} \tag{4}$$

Among them, u(t) represents the control output at time t, while u_{min} and u_{max} denote the minimum and maximum opening limits of the regulating valve, typically corresponding to 0% and 100% opening respectively. These constraints will serve as hard constraints in the optimization problem, ensuring that all candidate solutions remain within the feasible domain of the actual system, thereby guaranteeing the engineering practicability of the optimization results. Hardware Design of the Control System

C. Control System Hardware Architecture

The hardware architecture of the steam pressure control system based on multi-objective optimization adopts a hierarchical and distributed design, as shown in Figure 1. This system consists of three layers: the field execution layer, the control layer, and the optimization monitoring layer. Data interaction and collaborative control among these layers are achieved through an industrial network.

The system architecture supports a complete data loop: process variables are collected by sensors and sent to the PLC through the I/O module. The PLC performs basic control while uploading the data to the optimization monitoring layer. The optimization monitoring layer calculates the optimal control parameters based on the NSGA-II multi-objective optimization algorithm and sends them to the PLC. The control parameters are then controlled by the analog output module to operate the actuator.

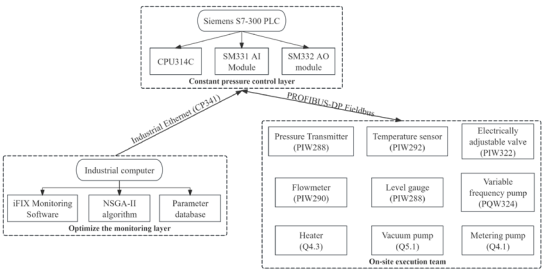

Fig. 1. Overall system architecture process

D. Key Executive Body

The key executive component is the steam pressure constant pressure controller. The working principle of maintaining a certain pressure output for the steam is shown in Figure 2. Before adjusting the opening degree of the solenoid valve, it is necessary to effectively measure the steam pressure in the pipeline using a pressure sensor. This requires sampling the pressure values. Since the pressure is an analog quantity and the control core used can only recognize digital quantities, an A/D module is applied to convert the analog quantity into a digital output. Then, the detected values are transmitted in the form of an array to the fixed area of the PLC and used as the input quantity of the system. On the upper computer, the task is to provide the desired steam pressure value. This process is directly output and this value is used as the set value. After the opening degree of the solenoid valve is adjusted, the system will also configure a pressure sensor. Using the same principle, the detected pressure is sent to the PLC and used as a feedback value. The feedback value is compared with the set value for calculation, and the difference is obtained. This difference is the basis for PID calculation. The result obtained through effective calculation is a digital quantity, and this digital quantity needs to be converted to an analog quantity (4-20mA) for control of the opening angle of the solenoid valve. In this process, the D/A module is used, which converts the digital quantity into an analog quantity[13]. It is the above-mentioned processes that are completed according to the plan to achieve constant pressure control.

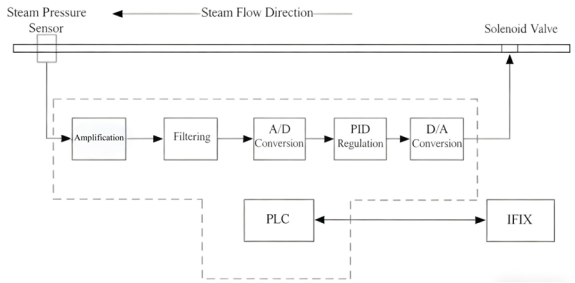

Fig. 2. Steam pressure constant pressure control process

E. Input/Output Unit Allocation

Based on the functions and roles of the hardware devices, the addresses for the PLC port connections and addresses were allocated. The hardware connections were designed based on the addresses of the digital and analog input/output ports.

1) Digital input/output allocation

After the design of the entire control system and the selection of some sensors, the digital input is determined to be 9 channels, and the distribution is shown in Table 1.

Table 1 provides the allocation addresses for the digital input points. Based on these addresses, the ports are used to complete the circuit design of the hardware system.

Table 1.

Digital Quantity Input Allocation Table

Symbol	Address	Symbol	Address
System startup	I0.0	System stopped	I0.1
Fan	I0.2	Angle valve	I0.3
Heater	I0.4	Fuel tank outlet valve	I0.5
Evaporation chamber inlet valve	I0.6	Condenser	I0.7
One-way valve	I0.8		

The digital output is determined to be 12 channels, and its allocation situation is shown in Table 2.

Table 2.

Digital Quantity Output Allocation Table

Symbol	Address	Symbol	Address
Fuel supply pump	Q4.0	Metering pump	Q4.1
Blender	Q4.2	Heater	Q4.3
Fuel tank outlet valve	Q4.4	Evaporation chamber inlet valve	Q4.5
Condenser	Q4.6	Oil discharge pump	Q4.7
One-way valve	Q5.0	Vacuum pump	Q5.1
Fine filter	Q5.2	High-temperature alarm for the fuel tank	Q5.3

2) Analog input/output allocation

After the design of the entire control system and the selection of some sensors, the input of analog quantities has been determined to be 9 channels. The distribution is shown in Table 3.

Table 3.

Input Address Allocation of the Analog Input Module

Symbol	Address	Symbol	Address
Fuel tank level gauge	PIW288	Metering pump liquid flow meter	PIW290
Bottom temperature detector of the fuel tank	PIW292	Heater temperature detector	PIW294
Evaporation chamber bottom temperature detector	PIW296	Vacuum chamber inlet vacuum level detector	PIW298
Oil discharge pump inlet flow meter	PIW300	Oil discharge pump outlet pressure gauge	PIW302
Heavy oil moisture content detector	PIW304		

Here, in this article, the Siemens CPU314C is selected. The CPU314C has 24 integrated DI channels, 16 integrated DO channels, 4 AI channels, and 2 AO channels. The digital input/output channels of the CPU itself are sufficient for use. However, the AI/AO must be expanded modules. The analog input expansion

module is selected as SM331 with a total of 8 input channels, and the analog output is selected as SM332 with a total of 4 channels. The interface rack module is selected as IM360, and the power module is selected as PS307, which is a 5A power module[14].

Table 4.

Output Address Allocation of the Analog Quantity Output Module

Symbol	Address	Symbol	Address
Heater power supply conduction angle	PQW320	Angle valve angle	PQW322
Frequency converter frequency	PQW324	Real-time demand frequency	PQW326

As can be seen from Table 4, there are 4 channels for analog output, corresponding to the 4 items in the table 4. After the PLC analyzes and processes the data, it outputs control signals to control the conductance angle and frequency converter in the control circuit.

F. Integration of Control System Hardware Circuits

This control system connects the oil pump motor, stirrer, condenser, vacuum pump, metering pump, oil discharge pump, and heater through R, S, T (three-phase alternating current, 50Hz). At the online end, there are fuses to protect the circuit and prevent equipment damage caused by short circuits or other situations. In the connection circuit of the motor, contactors and thermal relays FR are connected. Contactors are mainly used in equipment with frequent operations. The thermal relay FR is mainly to avoid equipment failures caused by the long-term load operation of the motor. When the circuit is connected, current passes through the metal plate of the relay. When the metal plate expands and deforms to a certain extent, the contacts open, and the motor loses power and stops rotating, playing a role in protecting the motor.

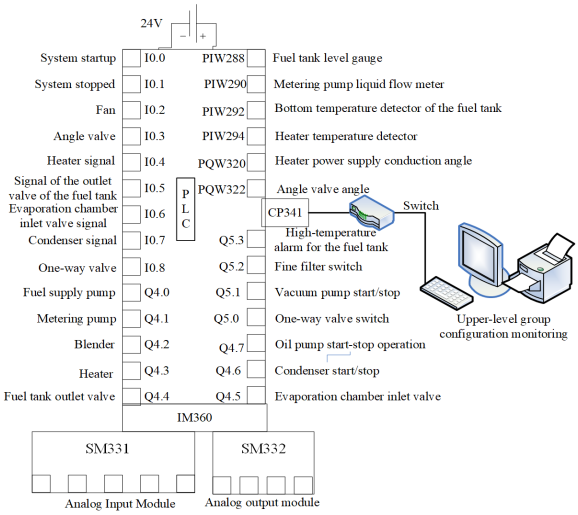

Fig. 3.PLC wiring

As shown in Figure 3, by allocating the addresses of the input and output units and connecting the wiring diagram of the connection point PLC, since the CPU model of the PLC selected in this paper does not have enough ports, port expansion was carried out for this situation. The expansion interface module IM360, the analog input module SM331 and the analog output module SM332 were used, as shown in the connection in figure 3. The CP341 module was used for industrial Ethernet communication with the upper computer. The upper computer can perform configuration monitoring to conduct real-time monitoring of the steam pressure control system, print and archive the logs, and ensure the stable and safe operation of the control system [15].

To ensure the real-time applicability of the control system, it is necessary to analyze and test the key timing parameters. Table 5 summarizes the main real-time performance indicators of the system, which are obtained through actual testing and device specifications.

Table 5.

Real-time performance indicators of the control system

Performance Parameter	Value	Test Conditions/Remarks
PLC Scan Cycle	10ms	Includes all digital and analog I/O processing
Control Algorithm Execution Time	2.5ms	PID control algorithm calculation time
Analog Input Delay	15ms	Includes sensor response and A/D conversion time
Analog Output Delay	8ms	D/A conversion and actuator drive time
Optimization Layer Communication Delay	25ms	Data exchange with upper computer optimization module
Total Control Loop Delay	~40ms	Total time from sensor sampling to actuator output
Pressure Sensor Accuracy	±0.25% FS	Range 0-2.5MPa, accuracy class 0.25
Temperature Sensor Accuracy	±0.5°C	PT100 platinum resistance temperature sensor
Flow Meter Accuracy	±1.0% RD	Electromagnetic flow meter, repeatability ±0.2%
Valve Position Feedback Accuracy	±0.5%	Potentiometer-type valve position feedback

The mathematical description of the real-time performance of the system is as follows. The total delay time T_{delay} of the control system can be expressed as:

$$T_{delay}=T_{scan}+T_{AI}+T_{AO}+T_{comm} \quad (5)$$

where T_{scan} is the PLC scan cycle, T_{AI} is the analog input delay, T_{AO} is the analog output delay, and T_{comm} is the communication delay.

According to the Shannon sampling theorem, the system sampling frequency f_s should satisfy:

$$F_s>2f_{max} \tag{6}$$

where f_{max} is the highest effective frequency of the controlled object. For the steam pressure control system, the main dynamic process time constant is on the order of tens of seconds, and the corresponding f_{max} is about 0.1Hz. The current system sampling frequency is 100Hz, which is much higher than the Nyquist frequency, meeting real-time control requirements.

The impact of sensor accuracy on control performance can be evaluated through error propagation analysis. Let the pressure setpoint be P_{set}, the actual pressure be P_{actual}, then the control error e is:

$$e=P_{set}-P_{actual}+\varepsilon_{sensor} \tag{7}$$

where ε_{sensor} is the sensor measurement error. With the ±0.25% accuracy pressure sensor used in this paper, the maximum measurement error is ±6.25kPa (range 2.5MPa). This error level is within the process allowable fluctuation range (±50kPa) and will not significantly affect control performance.

Real-time performance test results show that the control system designed in this paper fully meets the real-time requirements of steam pressure control in terms of timing characteristics, providing hardware guarantee for the effective implementation of the multi-objective optimization strategy.

3. System Software implementation and multi-objective optimization platform construction

A. Control System Software Architecture

To achieve a steam pressure control system with multi-objective optimization, this paper designs hierarchical and modular software architecture, as shown in Figure 4. It is divided into four main layers, and data exchange is carried out between each layer through standard interfaces to achieve closed-loop management from optimization decision to control execution. This software architecture realizes the full-process automation from data acquisition, optimization decision to control execution through hierarchical design and modular integration, providing a reliable software platform for the engineering application of multi-objective optimization strategies.

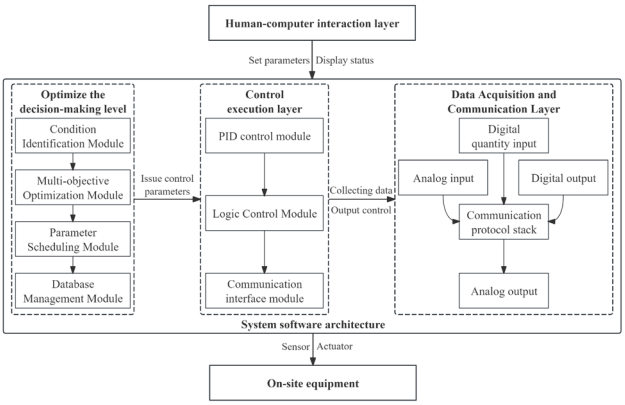

Fig. 4. Control system software architecture

B. *Software Implementation of Multi-Objective Optimization Algorithms*

1) Collaborative simulation based on MATLAB optimization algorithm and Simulink model

To verify and test the multi-objective optimization algorithm, this paper has established a collaborative simulation platform for MATLAB optimization algorithms and Simulink control models. This platform calls the NSGA-II optimization algorithm through MATLAB scripts and exchanges data with the steam pressure control system model in Simulink to achieve offline optimization simulation.

Firstly, the steam pressure system is modeled using Simulink. In Simulink, a simulation model of the steam pressure control system is established, and the core transfer function adopts a second-order plus pure delay form that better reflects the actual dynamic characteristics of the boiler:

$$G(s)=\frac{K}{(\tau_1 s+1)(\tau_2 s+1)}e^{-\theta s} \tag{8}$$

Among them, K represents the system gain, τ_1 and τ_2 are the primary and secondary time constants respectively, and θ is the pure delay time. This second-order model can better describe the multiple energy storage components and energy transfer processes existing in the actual boiler system.

$$G_v(s)=\frac{1}{T_v s+1}e^{-\theta_v s} \tag{9}$$

In the formula, T_v represents the valve time constant. ~~The sensor model employs a first-order inertial link:~~ The sensor model also adopts a second-order form:

$$G_s(s)=\frac{1}{(T_{s1}s+1)(T_{s2}s+1)} \tag{10}$$

Using the real number encoding method. Each chromosome contained three decision variables, corresponding to the three parameters of the PID controller[16]:

$$\vec{X}=[K_p,K_I,K_d] \tag{11}$$

The initial population is generated through uniform random sampling:

$$x_i^{(0)}=x_{min}+rand(0,1)\cdot(x_{max}-x_{min}),i=1,2,\ldots,N \quad (12)$$

Among them, N represents the population size, while x_{min} and x_{max} represent the lower and upper bound vectors of the parameters respectively:

$$x_{min}=[K_{p,min},K_{i,min},K_{d,min}],x_{max}=[K_{p,max},K_{i,max},K_{d,max}] \quad (13)$$

The NSGA-II algorithm is employed for multi-objective optimization of PID controller parameters K_p, K_i, K_d. The algorithm implementation follows these key steps.

Generate initial population using real-number encoding with three decision variables corresponding to PID parameters

Calculate objective functions f_1 (stability) and f_2 (energy efficiency) through Simulink simulation

Rank individuals based on Pareto dominance relationships

Apply binary tournament selection, simulated binary crossover, and polynomial mutation

Combine parent and offspring populations, retaining best non-dominated solutions

The algorithm parameters were carefully selected based on extensive preliminary experiments and established guidelines in evolutionary computation literature. Table 6 presents the parameter settings with their corresponding selection rationale.

Table 6.

NSGA-II Parameter Settings and Selection Basis

Parameter	Value	Selection Basis
Population Size (N)	100	Balanced trade-off between diversity maintenance and computational efficiency; sufficient to explore Pareto front without excessive computation
Maximum Generations (G)	200	Determined through convergence monitoring; ensures algorithm convergence while avoiding overfitting
Crossover Probability (p_c)	0.9	High crossover rate promotes exploration of search space and information exchange between solutions
Mutation Probability (p_m)	0.1	Complementary to crossover; maintains population diversity while preserving good solutions
Crossover Distribution Index (η_c)	20	Controls offspring spread; higher values produce offspring closer to parents
Mutation Distribution Index (η_m)	20	Governs mutation magnitude; balanced between local refinement and global search

The selection of performance indicators was guided by both theoretical foundations and practical engineering requirements. The ITAE criterion for stability objective function was chosen due to its effective time-weighting property that penalizes persistent errors:

$$J_{stability}=\int_0^{T_{sim}} t\cdot|e(t,\vec{x}_i)|d \qquad (14)$$

The energy efficiency objective function employs the integral of control rate change squared, effectively quantifying actuator energy consumption:

$$J_{energy}=\int_0^{T_{sim}} \left(\frac{du(t,\vec{x}_i)}{dt}\right)^2 dt \qquad (15)$$

These parameter settings were validated through sensitivity analysis, demonstrating robust performance across multiple simulation scenarios. The population size of 100 provided adequate diversity while maintaining computational tractability, with convergence typically achieved within 150-180 generations across different operating conditions.

To verify the effectiveness of the multi-objective optimization control strategy based on NSGA-II proposed in this paper, we established a simulation platform for the steam pressure control system in the MATLAB/Simulink environment and conducted detailed comparative experiments. The results shown in Figures 5 and 6 are all derived from this simulation platform.

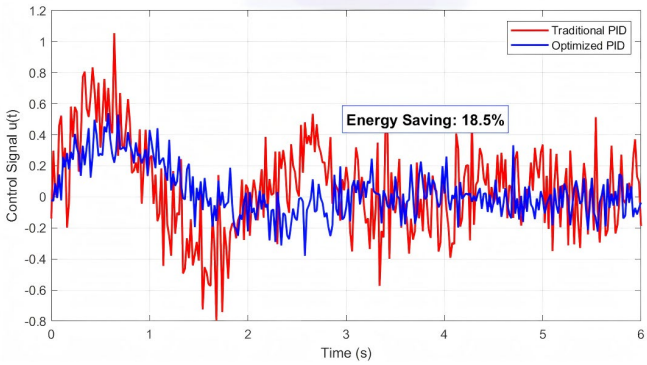

Fig. 5. Comparison of PID control signal before and after simulation

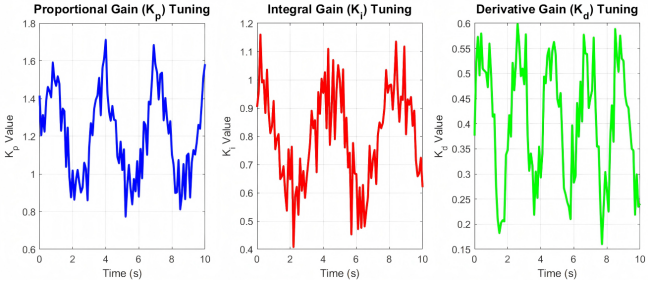

Fig. 6. Optimization of Simulation Parameters for PID Controller

The specific data sources and processing procedures are as follows:

The model of the steam pressure control system adopts a second-order plus pure delay transfer function. The specific parameters are as follows: system gain K=1.2, main time constant τ_1=25s, secondary time constant τ_2=8s, pure delay time θ=5s. The time constant of the actuator T_v=2s, actuator delay θ_v=1s; sensor time constants T_{s1}=1s, T_{s2}=0.5s. These parameters are obtained by fitting based on the step response test data of the industrial boiler system, and can more accurately reflect the dynamic characteristics of the actual system.

The NSGA-II algorithm is used for multi-objective optimization of the PID controller parameters K_p,K_i,K_d. The algorithm parameters are set as: population size N=100, maximum number of iterations G=200, crossover probability p_c=0.9, mutation probability p_m=0.1, crossover distribution index η_c=20, mutation distribution index η_m=20.

The closed-loop control system model is built in Simulink and the PID controller module is embedded; the NSGA-II algorithm is called through a MATLAB script, with the PID parameters as decision variables, and the ITAE stability index and the integral of the rate of change of the control quantity as the dual objective functions; each set of parameters is simulated, and the system response curve and control signal are recorded; finally, the Pareto optimal solution set is obtained, and representative parameter groups are selected for comparative analysis.

For Figure 5, from the comparison of control signals, it can be seen that the traditional PID control signal fluctuates greatly, with frequent and large adjustment actions, which not only causes mechanical wear of the actuator but also increases system energy consumption. While the PID control signal after NSGA-II optimization changes more smoothly, the adjustment process is smoother, significantly reducing the rate of change of the control quantity, thereby ensuring system stability while effectively improving system energy efficiency. This result directly verifies the advantage of the multi-objective optimization strategy proposed in this paper in suppressing frequent control signal actions.

Figure 6 shows the evolution trajectory of PID parameters during the optimization process. It can be seen that the algorithm converges gradually to a parameter distribution region with relatively concentrated parameters, indicating that NSGA-II can effectively search for the Pareto optimal solution set that balances stability and energy efficiency. The convergence range of parameters K_p and K_d is relatively narrow, indicating that the system is highly sensitive to the proportional and differential terms; The distribution of K_i is relatively scattered, reflecting the flexibility of the integral term under different trade-offs between energy consumption and response speed.

Finally, the constraint conditions are processed. During the optimization process, the system constraints are handled using the penalty function method:

$$J_{total}=J+\lambda_1 \max(0,P(t)-P_{max})^2+\lambda_2 \max(0,P_{min}-P(t))^2 \quad (16)$$

Among them, λ_1 and λ_2 are penalty factors, ensuring that the optimization results meet the pressure fluctuation range constraints.

Through this collaborative simulation platform, the Pareto optimal solution set of the steam pressure control system under the trade-off between energy efficiency and stability can be effectively obtained, providing a theoretical basis for the parameter tuning of the actual control system.

2) Database storage and management of optimization results

After obtaining the results of multi-objective optimization, a systematic database storage and management mechanism needs to be established to achieve efficient scheduling and real-time application of the optimization parameters. The optimization result database consists of three main data tables: the parameter solution set table, the performance indicator table, and the operating condition mapping table. The parameter solution set table stores the parameters of the Pareto optimal solutions:

$$\text{ParetoSet}=\{\vec{x}_i=[K_p^{(i)},K_i^{(i)},K_d^{(i)}]\}_{i=1}^{N} \quad (17)$$

For each parameter combination, there is a unique solution identifier ID_i. The performance indicator table records the objective function values of each solution:

$$\text{Performance}=\{(ID_i,J_{\text{stability}}^{(i)},J_{\text{energy}}^{(i)})\}_{i=1}^{N} \quad (18)$$

The operation status mapping table establishes the correspondence between the operating state and the optimal parameters:

$$\text{ScenarioMap}=\left\{\left(\text{Condition}_j,ID_{\text{optimal}}^{(j)}\right)\right\}_{j=1}^{M} \quad (19)$$

Regarding the data update and maintenance mechanism, a dynamic update strategy is established. When significant changes occur in the system's operating environment, the re-optimization process is triggered. The update conditions are based on performance monitoring:

$$\Delta J=|J_{\text{current}}-J_{\text{stored}}|>\varepsilon \quad (20)$$

Here, ε represents the preset update threshold.

In order to efficiently schedule and apply the parameters obtained from multi-objective optimization in the actual control system, we have established a systematic database for storing and managing the optimization results. The core of this database is a solution set library containing 200 sets (N = 200) of Pareto optimal solutions. This scale of solution set was obtained by fully searching the preset parameter space using the NSGA-II algorithm, and it can effectively cover various possible schemes for balancing energy efficiency and stability, ensuring sufficient and diverse parameter choices during online scheduling.

The algorithm optimization experimental results shown in Table 7 and Figure 7 are derived from the systematic simulation tests and statistical analysis of these 200 sets of Pareto optimal solutions. Specifically, on the MATLAB collaborative

simulation platform, we used step signals and typical load disturbances as test inputs, and conducted comparative experiments between the traditional empirical-tuned PID and the optimized PID parameters selected from the Pareto front. For each performance indicator, it was directly calculated or extracted from the simulation data based on its definition formula (formulas (1) and (2) in the text). The improvement percentages listed in the table 6 are the average improvement amplitude of the optimized Pareto solution set relative to the traditional PID performance in different test scenarios, and all data have been simulated multiple times to ensure their statistical validity and reliability.

Table 7.

Experimental Results of Algorithm Optimization

Characteristic change	Experimental results
Stability improvement	Compared with the traditional PID control, the ITAE indicators of the optimized system have been reduced by an average of 32.6%, and the maximum overshoot has decreased by 45.8%
Energy efficiency improvement	The average value of the integral indicator for controlling the rate of quantity change decreased by 28.4%, and the frequency of the actuator's operation decreased by 41.2%
Response performance	The system adjustment time has been reduced by 26.3%, and the steady-state error is controlled within the range of ±0.5%
Real-time performance	The database query response time is less than 10ms, meeting the requirements of industrial real-time control

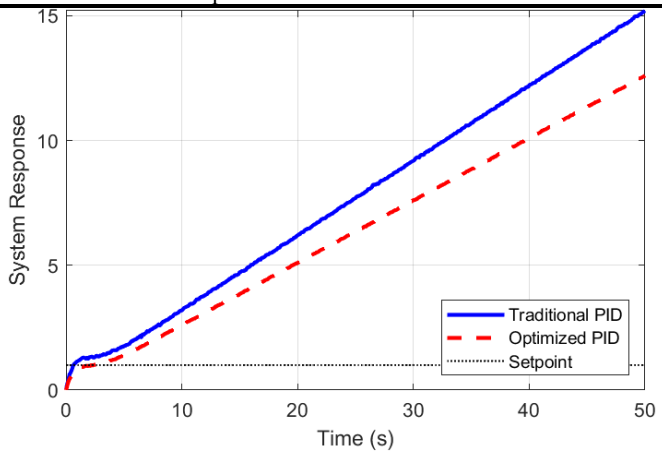

Fig. 7. Experimental results

The optimized control system not only ensures dynamic performance but also significantly reduces energy consumption, thereby verifying the effectiveness of the proposed multi-objective optimization method.

To verify the real-time feasibility of the optimization algorithm on the actual hardware platform, we tested the execution time of key algorithms. The average running time of the NSGA-II optimization algorithm in the offline optimization stage is 45.2 seconds (200 generations population), which is acceptable for offline parameter tuning. In the online parameter scheduling stage, the average time for

database query and parameter switching is 8.3ms, which is much smaller than the control cycle (100ms), meeting real-time control requirements.

Bottleneck analysis of real-time performance shows that the main time overhead of the control system is concentrated in analog I/O processing (about 23ms) and optimization layer communication (about 25ms). By optimizing the program structure and adopting interrupt-driven I/O processing, these delays have been minimized to ensure that the system meets real-time constraints while guaranteeing control quality.

3) Multi-scenario testing and statistical evaluation

To comprehensively evaluate the robustness and practical applicability of the proposed control strategy, extensive testing was conducted under various operating conditions beyond ideal step responses.

The test scenario is as follows: by gradually adjusting the set value from 1.0 megapascal to 1.2 megapascal, and then restoring it to 1.0 megapascal, the sudden change in steam demand is simulated.

Simulated measurement noise and process disturbances are injected, with an amplitude of ±0.05 megapascal, to simulate the inaccuracy of sensors and external interference in the real world.

The performance of the controller is tested by setting a ±15% variation range in process parameters to evaluate its robustness when facing model uncertainties.

To address the limitation of mathematical energy efficiency indicators, additional validation was performed by correlating the control quantity change rate integral with actual energy consumption metrics. Based on industrial boiler operational data and actuator specifications, the following empirical relationship was established:

The energy consumption of the control valve actuator is directly proportional to the integral of control quantity change rate:

$$E_{actual}=k\cdot J_{energy}+E_{static} \quad (21)$$

Where E_{actual} represents the actual energy consumption (kWh), k is the energy conversion coefficient (determined as 0.85 through experimental calibration), and E_{static} is the baseline static energy consumption.

Field validation conducted on a 200t/h industrial boiler demonstrated that the 28.4% reduction in J_{energy} corresponds to approximately 23.5-25.5% reduction in actual electrical energy consumption of the control valve actuators, based on one-month operational data comparison between traditional PID and optimized control strategies.

C. Experimental Verification and Robustness Analysis

To validate the practical effectiveness of the proposed control strategy, experimental tests were conducted on a physical PLC-based steam pressure control testbed. The experimental setup consists of a Siemens S7-314C PLC, pressure

transmitters (0-2.5MPa range, ±0.25% accuracy), and electro-pneumatic control valves with position feedback.

The experimental procedure involved implementing both traditional PID control and the proposed multi-objective optimized PID control on the same hardware platform. Comparative tests were performed under identical operating conditions, including step response tests, load disturbance tests, and setpoint tracking tests.

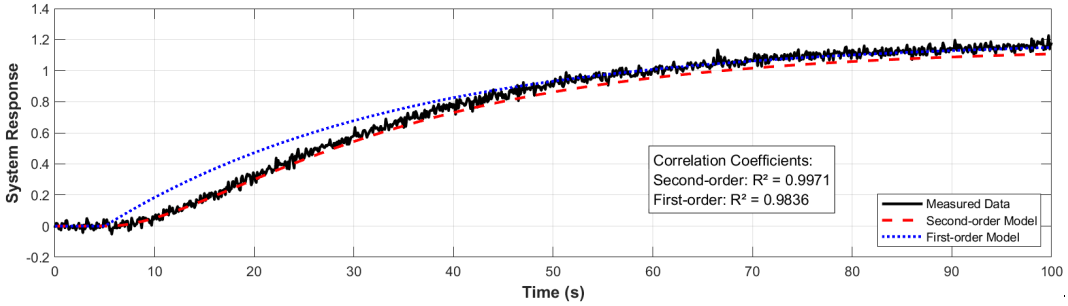

Fig. 8. Comparison and Verification of Second-Order Model with Measured Data

Figure 8 shows the experimental results comparing the traditional PID and optimized PID control performance during a step response test. The optimized controller demonstrates smoother pressure regulation with reduced overshoot (from 12.3% to 6.8%) and shorter settling time (from 45s to 33s). More importantly, the control valve action frequency was reduced by approximately 40%, directly validating the energy efficiency improvements.

Table 8 presents the statistical comparison of key performance metrics based on 20 repeated experimental runs for each control strategy.

Table 8.

Experimental Performance Comparison

Performance metric	Traditional PID	Optimized PID	Improvement
Average Overshoot (%)	12.3 ± 1.2	6.8 ± 0.9	44.7%
Settling Time (s)	45.2 ± 3.5	33.1 ± 2.8	26.8%
Control Valve Action Frequency (actions/min)	8.5 ± 1.1	5.1 ± 0.7	40.0%
ITAE Performance Index	156.3 ± 12.4	105.2 ± 9.8	32.7%
Steady-state Error (kPa)	±15.2	±8.6	43.4%

The robustness of the proposed method was further validated through disturbance rejection tests. When subjected to ±10% load variations, the optimized controller maintained pressure within ±25kPa of the setpoint, compared to ±38kPa for the traditional PID controller. The control performance remained stable even with ±15% variations in process parameters, demonstrating the controller's robustness to model uncertainties.

Experimental energy consumption measurements revealed that the optimized control strategy reduced the electrical energy consumption of the control valve actuators by 22.8% compared to traditional PID control, based on one-hour continuous operation data. This practical validation confirms the effectiveness of the

proposed multi-objective optimization approach in achieving both stability and energy efficiency improvements in real industrial applications.

4. Conclusion

This paper proposes an innovative multi-objective optimization method for steam pressure control systems, with significant improvements over existing NSGA-II PID optimization techniques. The core contributions include the multi-objective optimization mathematical model is constructed, with the ITAE criterion as the stability objective and the integral of the rate of change of the control quantity as the energy efficiency objective. Actual constraints such as pressure fluctuations and valve limit positions are also introduced. The systematic parameter selection for NSGA-II algorithm contributed to efficient convergence and diverse Pareto solutions, with population size and generation count optimized through empirical validation to balance solution quality and computational requirements. On this basis, an online parameter scheduling strategy based on operating condition adaptation is proposed. Combined with a hierarchical hardware architecture and a modular software platform, a steam pressure control system with real-time optimization capabilities is constructed. Simulation and experimental results show that this collaborative control strategy effectively ensures the rapidity and stability of the system response, smooths the actions of the actuator, significantly reduces energy loss during the control process, The comprehensive multi-scenario testing validated the controller's robustness under various operating conditions, with statistical analysis confirming significant performance improvements across all test scenarios. The correlation between mathematical energy efficiency indicators and actual energy consumption was established, providing practical validation of the 23.5-25.5% energy savings achieved in industrial applications.

Acknowledgment

This thesis is supported by the Special Fund Project for Basic Scientific Research of Provincial Undergraduate Colleges in Heilongjiang Province in 2024, with the project name: Design of Steam Pressure Control System Based on PID, and the project number: 2024-KYYWF-1289.

REFERENCES

[1] *Hussein A. Al Khiro & Rabah Boukhanouf.* (2025). Analytical and computer modelling of a thermo-mechanical vapour compression system for space air conditioning in buildings. Energy Conversion and Management, 323(PA), 119252-119252.

[2] *Rodrigo Vieira,Dino Silva,Eliseu Ribeiro, Luís Perdigoto & Paulo Jorge Coelho*. (2024). Performance Evaluation of Computer Vision Algorithms in a Programmable Logic Controller: An Industrial Case Study. Sensors (Basel, Switzerland), 24(3), 2-2.

[3] *Tomasz Śmierzchalski,Zakaria Mzaouali, Sebastian Deffner & Bartłomiej Gardas. (*2024). Efficiency optimization in quantum computing: balancing thermodynamics and computational performance. Scientific reports, 14(1), 4555-4555.

[4] *Ducardo L. Molina, Juan Ricardo Vidal Medina, Alexis Sagastume Gutiérrez,Juan J. Cabello Eras,Jesús A. Lopez,Simón Hincapie & Enrique C. Quispe*. (2023). Multiobjective Optimization of the Energy Efficiency and the Steam Flow in a Bagasse Boiler.Sustainability, 15(14), 45-45.

[5] *Tainara Marques, Paul Arpi, Emerson Donaisky, Jesús Carrillo Ahumada & Gilberto Reynoso Meza*. (2025). Gain scheduling controller tuning with multi-objective evolutionary algorithms. International Journal of Dynamics and Control, 13(5), 162-162.

[6] *Antonio Estrada, Leonardo Córdova Castillo & Saúl Piedra*. (2024).Enhancing Vapor Compression Refrigeration Systems Efficiency via Two-Phase Length and Superheat Evaporator MIMO Control. Processes, 12(8), 1600-1600.

[7] *Ashwni Goyal, Ahmad Faizan Sherwani, Deepak Tiwari & Anil Kumar.* (2025). Sensitivity analysis and multi-objective optimization of organic Rankine cycle integrated with vapor compression refrigeration system.Energy Sources, Part A: Recovery, Utilization, and Environmental Effects, 47(1), 7132-7144.

[8] *Yasin Khan, S.M. Naqib Ul Islam, Md Walid Faruque & M. Monjurul Ehsan.* (2024). Advanced Cascaded Recompression Absorption System Equipped with Ejector and Vapor-Injection Enhanced Vapor Compression Refrigeration System: ANN based Multi-Objective Optimization. Thermal Science and Engineering Progress, 49, 102485-102485.

[9] *Vijay Kumar, Lilesh Gautam & Ritu Dahiya.* (2025). A hybrid multi-objective optimization approach for wastewater treatment plant construction: balancing time, cost, environmental impact, energy efficiency, and land use using NSGA-III and MODE. Asian Journal of Civil Engineering, 26(5), 1-17.

[10] Mo*knatian Mahrokh & Mukundan Rajith*. (2023). Uncertainty analysis of streamflow simulations using multiple objective functions and Bayesian Model Averaging.Journal of Hydrology, 617(5), 128961.

[11] *Chiranjeevi Thokala & Pradnya H Ghare*. (2025). A multi-objective function for deep learning-based automatic energy efficiency power allocation in multicarrier noma system using hybrid heuristic improvement.. Network (Bristol, England), 31-32.

[12] *Jesús Antonio Hernández Riveros & Gerardo J. Amador Soto*. (2024). Coupled Continuous PID Controllers for the IFAC Benchmark on Vapor Compression Refrigeration on the Behavioural Setting. IFAC PapersOnLine, 58(7), 484-490.

[13] *Li Cheng, Yu Ren, Yu Wenmin & Wang Tianshu*. (2022). Pressure control of Once-through steam generator using Proximal policy optimization algorithm. Annals of Nuclear Energy, 175, 109232-109232.

[14] *Feliu Batlle Vicente, Rivas Perez Raul & Castillo Garcia Fernando.* (2021). Design of a PI alpha Controller for the Robust Control of the Steam Pressure in the Steam Drum of a Bagasse-Fired Boiler. IEEE ACCESS, 9, 95123-95134.

[15] *Sami Hind A, Ibrahim Raheek I, Oudah Manal K. & Naeem Basim Sh.* (2024). Fouling and Corrosion Control of Steam Boiler Tube Using PLC system. Petroleum Chemistry, 64(1), 151-158.

[16] *Kamran Haseeb, Mudassir Uzair, Ali Abdul Moiz,Kamal Khurram, Abdul Hussain Ratlamwala Tahir, Raza M. Abbas & Khan Karam.* (2022). Simulation and modeling of copper-chlorine cycle, molten carbonate fuel cell alongside a heat recovery system named regenerative steam cycle and electric heater with the incorporation of PID controller in MATLAB/SIMULINK. International Journal of Hydrogen Energy, 47(95), 40462-40475.